

MECHANISMS OF NUCLEATE POOL BOILING ON COMPOSITE SURFACES

G. W. Yang, Wen-Jei Yang and N. Zhang
Department of Mechanical Engineering and Applied Mechanics
University of Michigan, Ann Arbor, Michigan 48109

(Communicated by J.P. Hartnett and W.J. Minkowycz)

ABSTRACT

A previous experimental study [1] has disclosed that nucleate pool boiling heat transfer coefficients on a graphite-copper composite surface are three to six times higher than those on a pure copper surface. Three programs are executed in order to explore the cause for such a high thermal performance: An experiment is conducted on nucleate pool boiling of R113 on a composite surface, a computer program is developed to determine the temperature distribution inside a composite cylinder heated from the lower end with incipient boiling on the upper end, and the microstructure of the composite surface is examined by means of a scanning electronic microscope (SEM). The computer results indicate that (i) Each fiber acts like a fin transporting higher heat flux, resulting in the composite body having a higher average temperature at any cross sections than that of a pure base material, and (ii) There exists a criterion for the tip of graphite fibers to function as a hot spot, i.e. a potential site for macro-bubble nucleation. The SEM discovers micro trenches and intermingled winding trails on the matrix surface between graphite fiber tips which may serve as the nucleation sites for micro-bubbles. The experiments in support of both hypotheses about the nucleation site.

Introduction

Since nucleate boiling can achieve a high heat flux with a small excess temperature, it has been employed in various energy conversion systems and in component cooling. Numerous studies on nucleate boiling have been reported and many special nucleate boiling geometries have become available commercially [2]. There are five major categories of structured boiling surfaces: attached promoters (AP), porous boiling surfaces (PBS), integrated roughness surfaces (IRS), micro configuration enhanced surfaces (MES), and composite enhanced surfaces (CES). In the AP type, nucleation promoters are attached or bonded to the base surface. The PBS is a coated surface whereby an irregular matrix, either metal or nonmetal, of potential nucleation sites is produced by such methods as poor welding, sintering or brazing of particles, electrolytic decomposition and others. The IRS is formed by mechanical working of the boiling surface to produce I-type fins, T-type fins, Y-type fins or compressed saw-tooth type fins. These three

nucleate boiling geometries have one thing in common, that is, macro cavities (reentrant cavities, pores, or narrow reentrant channels) [3]. Consequently, they suffer from the same drawbacks: loss of enhancement efficiency due to fouling, pressure drop, and cost of fabrication and maintenance.

Recently, Gebhart and Wright [4] developed micro figured photo-etched silicon surfaces (MES). One geometry was hexagonal dimples (3.3 μm depth and 11.5 μm width) and the other was trenches (51 μm depth, 12 μm width and 100 μm length). In the nucleate boiling regime, these specimens achieved an average 3.9 times the heat dissipation predicted by general boiling correlation. Their experimental results showed no evidence of temperature overshoot associated with boiling hysteresis. France [5] and Miller and Gebhart [6] reported similar enhancement in nucleate boiling. The enhancement was attributed to the formation of high-frequency microbubbles on the microconfigured surfaces in addition to macro bubbles. Such a dual-bubble boiling mechanism would necessitate dual characteristic lengths and dual characteristic frequencies. Macro bubbles have a characteristic size of 0(1) mm and frequency of 0(100) Hz, while microbubbles possess a characteristic size of 0(10) μm and frequency of 0(10⁵) Hz. The arguments for the dual bubble boiling mechanism on the measured enhancement were that (i) Macrobubbles may have hidden micro bubbles which were formed in the liquid microlayer between the large bubble and the heated surface; and (ii) The microbubbles may have merged with the macrobubbles or perhaps, condensed and collapsed while still in the liquid microlayer underneath the macrobubbles. Therefore, the measured heat transfer was contributed not only by the macrobubbles but also by the microbubbles. Further studies are still needed to confirm the detailed mechanism which causes the measured enhancement.

The microconfigured geometries provide another technique to enhance boiling heat transfer by forming regular patterns of microcavities, analogous to the macrocavities formed on the PBS and IRS structures.

A recent study [7] classified the CES into two categories : discrete insert/matrix type composite and microfigured insert in matrix type composite. The former consisted of a copper plate as the base with triangular gutters inserted with Ni-Cr steel strips [8]. When the volume rate of the inserted material (Ni-Cr-Fe) to the base material (Cu) exceeded 25%, a plateau appeared in the boiling curve in the critical heat flux region accompanied by a reduction in the peak heat flux. It implies that the superheated region (i.e., safety region) with high heat flux is extended in the composite material compared with the base material. The variation in heat flux with surface temperature in the critical region becomes less sensitive in the composite material. No mention was made on the extent of heat transfer enhancement, however.

The Gr-Cu composite material to be studied here consists of graphite fibers of 10 to 15

μm embedded uniaxially within a copper matrix, by 50% volume fraction. With R-113 as the test liquid, the nucleate boiling heat transfer coefficients were 3 to 6 times those on the pure copper surface. Since the tips of the graphite fibers on the boiling surface are comparable to the size of nucleate boiling sites, they may have acted as nucleation sites. Another possible cause of the measured enhancement is the formation of microcavities on the composite surface. Three programs are offered in the present study to examine which of the two is responsible.

Program 1. Incipient Boiling Experiment

Figure 1 is a schematic of the test apparatus. It consisted of a copper block of 25 mm in diameter and 10 mm thickness which was embedded with only 30 graphite fibers in the

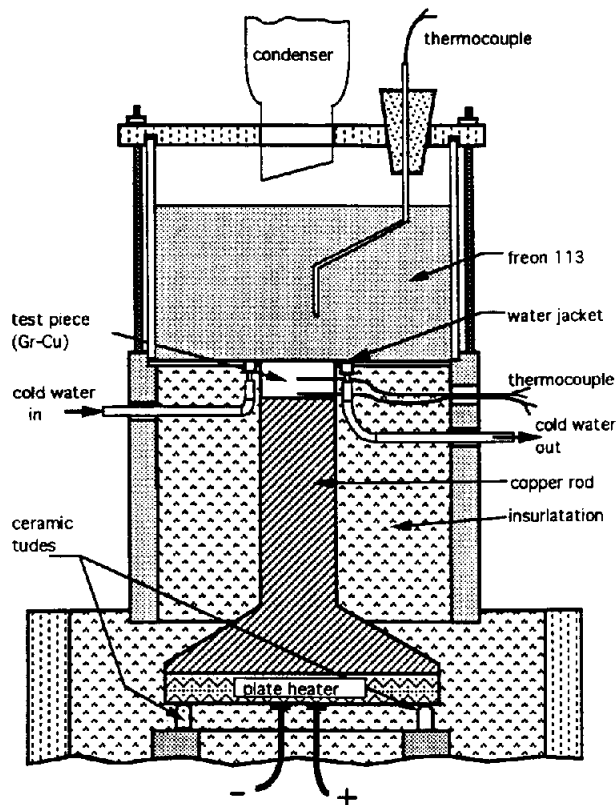


FIG. 1
Experiment set-up for nucleation sites verification
on a composite material surface.

axial direction. The distance between two adjacent graphite fibers is rather large compared with the size of each graphite fiber. Thus, there is no interaction among the graphite fibers. The

location of these fibers was detected by means of a scanning electronic microscope, as shown in Fig.2. The composite surface was heated underneath by a copper rod which was placed on a plate heater. Small ceramic tubes separated the plate heater from iron supporters to prevent heat loss by conduction. The periphery of the composite surface was silver-soldered to a copper water jacket for cooling to prevent boiling to occur there. The water jacket was joined to a thin stainless circular plate, with the gap filled with epoxy resin. The entire system was insulated by ceramic fiber.

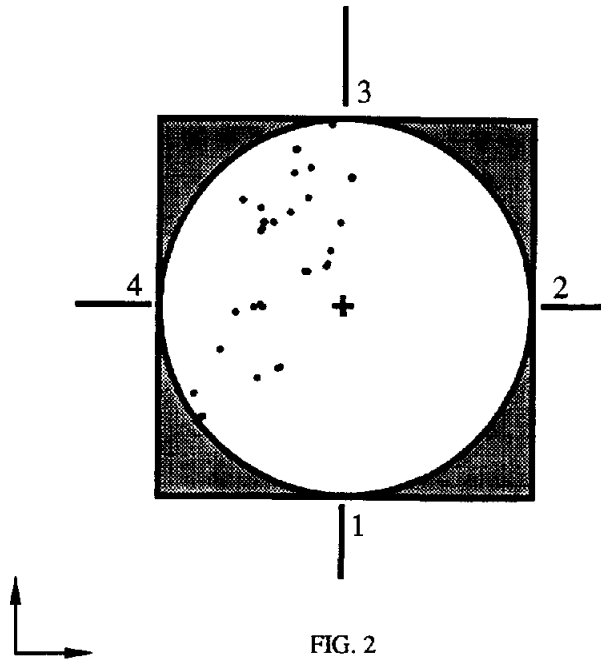


FIG. 2
Fiber location

A glass cylinder was placed on the edge of the stainless plate to form a space for boiling the test liquid, Freon 113. A condenser was mounted on the lid of the glass vessel to condense the vapor formed during a boiling test. The condensed vapor returned to the vessel by gravity. Two 40-gage copper-constantan thermocouples were installed inside the composite block along the axis. The boiling surface temperature was determined by a linear extrapolation of these two temperature readings. The boiling surface heat flux was also determined from these temperatures using the Fourier conduction law. A third similar thermocouple was placed 2 cm above the composite surface to monitor the bulk temperature of the test liquid. An electric strip heater was attached on the outer vessel surface to preboil the test liquid for degassing before each test. Incipient boiling tests were conducted on two composite surfaces with different roughnesses, being polished with 1- and 6- μm diamond abrasives. The test procedure is as follows:

The strip heater was turned off after one-half hour of degassing the test liquid. The power to the plate heater was then gradually raised, at 5 V increment, until the initiation boiling occurred. At each power setting, the system was permitted to stabilize for ten minutes. Subsequently, recordings were made on voltage, electric current, liquid pool temperature, and three thermocouple readings. During each test, the cooling water flow rate was adjusted in order to keep the edge not to exceed the boiling point of the test liquid. The situation on the composite surface under an incipient boiling state was recorded by a camera. The procedure was repeated for each run. The photographs of all test runs were carefully examined to see if bubbles appeared on the known positions of all graphite fiber tips.

Of all sixteen runs on the incipient boiling experiment, nucleation was observed on the area where no fiber was planted. No bubble was formed on the graphite fiber tips in this particular test sample.

Program 2. Computer Simulation

A computer program was developed to simulate heat transfer process in the composite block, shown in Fig.3, in which the length m can be adjustable, including $m = 0$. To simulate the incipient boiling, the temperature distribution on the heating surface was obtained using the highest natural heat transfer coefficient h . The objective of this program is to determine the condition for a graphite fiber tip to be a hot spot. The 3-D, steady heat conduction equation in the cylindrical coordinates (r, ϕ, z) reads

$$k_1 \frac{1}{r} \frac{\partial}{\partial r} \left(r \frac{\partial T}{\partial r} \right) + k_2 \frac{1}{r^2} \frac{\partial^2 T}{\partial \phi^2} + k_3 \frac{\partial^2 T}{\partial z^2} = 0 \quad (1)$$

where k_1 , k_2 and k_3 are thermal conductivities in the r , ϕ and z direction, respectively. For the copper matrix, $k_1 = k_2 = k_3 = k_m$. The appropriate boundary conditions are:

$$r \text{ direction: } \frac{\partial T}{\partial r} = 0 \quad (\text{at center and periphery}) \quad (2)$$

$$\text{base surface: } \frac{\partial T}{\partial z} = -\frac{q''}{k_3} \quad (3)$$

$$\text{top surface: } k_3 \frac{\partial T}{\partial z} + h(T - T_\infty) = 0 \quad (4)$$

Here, q'' denotes the heat flux from the plate heater. Equation (1) is discretized in the finite difference form using central-difference formula as

$$\begin{aligned} & \frac{k_1}{(\Delta r)^2} \left[\left(1 - \frac{1}{2i}\right) T_{i-1,j,k} + \left(1 + \frac{1}{2i}\right) T_{i+1,j,k} \right] \\ & + \frac{k_2}{i^2 (\Delta r)^2 (\Delta r)^2} (T_{i,j-1,k} + T_{i,j+1,k}) + \frac{k_3}{(\Delta r)^2} (T_{i,j,k-1} + T_{i,j,k+1}) \\ & - 2 \left[\frac{k_1}{(\Delta r)^2} + \frac{k_2}{i^2 (\Delta r)^2 (\Delta \phi)^2} + \frac{k_3}{(\Delta z)^2} \right] T_{i,j,k} = 0 \end{aligned} \quad (5)$$

The boundary conditions become

$$T_{i+1,j,k} = T_{i-1,j,k} \quad (6)$$

$$T_{i,j,k-1} = T_{i,j,k+1} + \frac{2\Delta z}{k_3} q'' \quad (7)$$

$$T_{i,j,k+1} = T_{i,j,k-1} - \frac{2\Delta z}{k_3} h(T_{i,j,k} - T_\infty) \quad (8)$$

They are the basic equations in the simulation of thermal behavior of the system. The expressions for the azimuthal boundary surface and graphite fiber can be derived based on the equations and are thus omitted here. Note that an equivalent thermal conductivity is employed in those equations for the graphite fiber nodes.

Numerical results were obtained for thermal behavior in four graphite composite structures with four different base materials: copper ($k=401$ W/m-k), aluminum ($k=204$ W/m-k), nickel ($k=90$ W/m-k), and stainless steel ($k=14.9$ W/m-k). Four different sizes of the graphite fiber were treated for each composite structure, with the diameter, d , of 0.335, 0.473, 0.754 and 0.946 mm. It is disclosed from the results that there is a relative temperature between the graphite fiber T_{Gr} and its surrounding base material T_b , depending on the distance from the base surface, z . The relative temperature is zero, i.e. $T_{Gr}=T_b$, at certain distance $z=\ell_c$. The graphite fiber has a lower temperature than the surrounding base material in the region where z is less than ℓ_c . For z exceeding ℓ_c , the relative temperature, $T_{Gr}-T_b$, is positive. However, the magnitudes of ℓ_c and $(T_{Gr}-T_b)$ depend on d , thermal property of the base material, and thermal resistance between the composite surface and the test liquid. ℓ_c is called "penetration depth" here. Fig. 4 plots the penetration depth against the fiber diameter for different base materials. Here, $h=1,200$ W/m²-k, $q''=1,500$ W/m², $T_\infty=47.0$ °C,..... The results indicate that stainless steel with the lowest thermal conductivity has the longest penetration depth, while copper with the highest thermal conductivity has the shortest penetration depth. The fiber tip can become a hot spot only if the composite structure has a thickness exceeding ℓ_c . Computer results indicate that the relative temperature may not increase with an increase in z but becomes equilibrated ($T_{Gr}-T_b=0$), depending on the base material. In the case of copper and aluminum with high thermal conductivities, the excess heat at a location in the graphite fiber due to the relative temperature can be easily dissipated through a base material of high thermal conductivity.

The graphite fiber tips in the composite structure that was tested in Program 1 have a

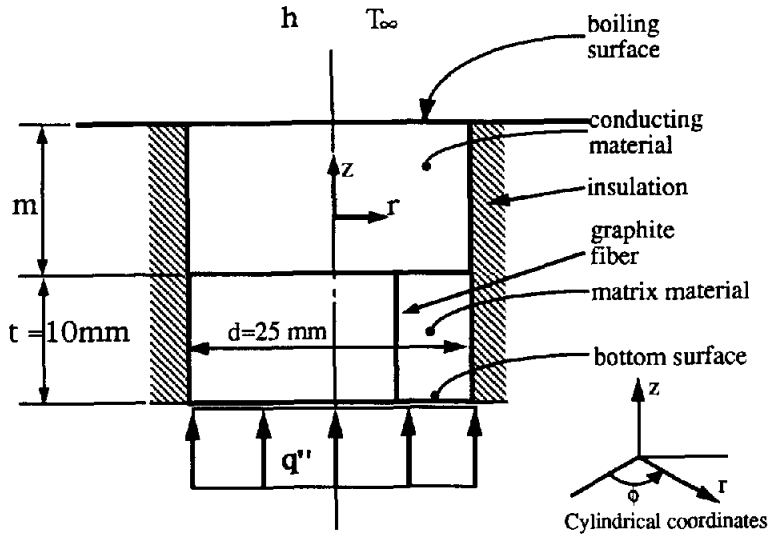


FIG. 3
A schematic representation of computer simulation for a specially made composite material.

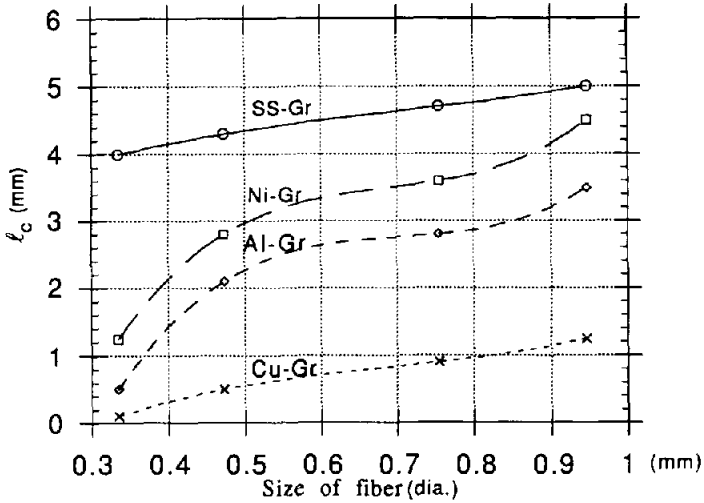


FIG. 4
Plot for temperature penetration

diameter of 10 to 15 μm and thus cannot possibly form hot spots. However, the formation of hot spots at graphite fiber tips may be possible if the thickness of the test specimen near but greater than its penetration depth ℓ_c is used or larger input of heat transfer rate is employed. Another important disclosure from the computer analysis is that the average temperature at any cross section (z) in the composite structure is higher than that in the pure base material of the same size and under the same operating conditions. It means that more energy can be extracted from an energy source by a material with graphite fibers embedded within. In other words, each fiber acts like a fin, making the graphite composite structures more efficient in transferring heat than the base materials.

Program 3. Surface Structure Scanning

The objective of this program is to examine the presence of microconfigurations on the composite surface which caused the measured enhancement [1]. First, the effect of hardness on surface roughness was tested on a graphite-copper composite of 50% volume fraction and a pure copper surface. Both surfaces were polished with 6 μm diamond abrasive and then measured by a profilometer. It was found that the mean square roughness (R_q) of the composite material (0.222 mm) was about 5 times that of pure copper (0.048 mm). Next, a scanning electronic microscope was used to scan the composite surface with a magnification of up to 10,000. It assured a perfect contact between the graphite fibers and the base material. Finally, a vacuum evaporation method was applied to coat a thin (about 0.2 μm) aluminum layer on the composite surface. An optical microscope was then used to examine the surface microstructure. Figures 5 (a) and (b) are photographs showing the microconfiguration on the composite surface. Each fiber tip appears as a plateau with rugged terrain, while the spaces (base material surface) between the plateaus are filled with a large number of micro-sized low-lying trenches and intermingled narrow grooves. These microconfigurations may act as nucleation sites. That is why the incipient boiling was seen to occur not on the fiber tips. With the fibers acting like fins to promote efficient heat conduction through the entire composite structure, the transient conduction process required for the bubble growth-departure cycle can be substantially reduced. It results in a higher bubble departure frequency which enhances nucleate boiling heat transfer performance, as reported in Yang et al. [1].

Conclusions

Three programs, incipient boiling experiment, computer simulation, and surface structure scanning have been executed to explain the mechanism of the measured enhancement in the nucleate boiling heat transfer performance on the graphite-copper composite surface. The



(a) 8000 Magnification



(b) 7900 Magnification

FIG. 5
Surface shape formed on the two selected graphite fiber tips

incipient boiling experiment has disclosed nucleation to begin not on the fiber tips but in the areas between them. The computer simulation has confirmed the experimental finding of no bubble formation on the fiber tips in this particular tested sample. It has disclosed that each graphite fiber acts like a fin, making the graphite composites more efficient in transferring heat than the base materials. The composite surface scanning has disclosed a large number of microsized low-lying trenches and intermingled narrow grooves. With these microconfigurations acting as the nucleation sites, a high bubble growth-departure cycle promoted by the efficient heat transfer through the composite structure can be responsible for the measured enhancement of nucleate boiling heat transfer performance.

Reference

- 1 Yang, W. J., Takizawa, H., and Vrable, D., *Int. J. of Heat and Mass Transfer*, **34**, no.11, 2751 (1991).
- 2 Webb, R. L., *Heat Transfer in Energy Problems* (eds. T. Mizushima and Wen-Jei Yang), Hemisphere, Washington D.C., 127 (1983).
- 3 Ralph, L. W., *Heat Transfer Engineering* **2** nos. 3-4 Jan-June, (1981).
- 4 Gebhart Benjamin and Wright Neil, *Int. Comm. Heat Mass Transfer*, **15**, no. 2, 141 (1988).
- 5 France, A. M., M. S. Thesis, University of Pennsylvania, Philadelphia, Pennsylvania (1989).
- 6 Miller, W. J. and Gebhart, B., to appear, (1992).
- 7 Yang, Wen-Jei and Zhang, Nengli., *Engineering Foundation Conference on Pool and External Flow Boiling*, Santa Barbara, CA., Mar. 23, 1 (1992).
- 8 Blagojevic, B. D., Novakovic, M. N., and Ilic, G. S., *Proceedings of The Ninth International Heat Transfer conference*, Jerusalem, Israel, **4**, 307 (1990).

Received July 8, 1992